FIELD AND CURRENT AMPLIFICATION IN THE SSPX SPHEROMAK*

D.N. HILL, R.H. BULMER, B.I. COHEN, E.B., HOOPER, H.S. MCLEAN, J. MOLLER, L.D. PEARLSTEIN, D.D. RYUTOV, B.W. STALLARD, R.D. WOOD, S. WOODRUFF, *Lawrence Livermore National Laboratory, Livermore, USA* hilld@llnl.gov

C.T. HOLCOMB AND T. JARBOE, *Univiversity of Washington, Seattle*

P. BELLAN AND C. ROMERO - TALAMAS, *California Institute of Technology, Pasadena, CA*

Abstract

Results are presented from experiments relating to magnetic field generation and current amplification in the SSPX spheromak. The SSPX spheromak plasma is driven by DC coaxial helicity injection using a 2MJ capacitor bank. Peak toroidal plasma currents of up to 0.7MA and peak edge poloidal fields of 0.3T are produced; lower current discharges can be sustained up to 3.5msec. When edge magnetic fluctuations are reduced below 1% by driving the plasma near threshold, it is possible to produce plasmas with Te > 150eV, $<\beta_e>$~4% and core χ_e~30m^2/s. Helicity balance for these plasmas suggests that sheath dissipation can be significant, pointing to the importance of maximizing the voltage on the coaxial injector. For most operational modes we find a stiff relationship between peak spheromak field and injector current, and little correlation with plasma temperature, which suggests that other processes than ohmic dissipation may limit field amplification. However, slowing spheromak buildup by limiting the initial current pulse increases the ratio of toroidal current to injected current and points to new operating regimes with more favorable current amplification.

1. Introduction

The spheromak is a unique, self-organized magnetized plasma configuration in which the confining magnetic fields are generated self-consistently by currents flowing within the plasma rather than by external coils [1]. Most commonly, a coaxial DC source (a Marshall gun) injects magnetic helicity into a cylindrical flux-conserving vessel where reconnection and other MHD processes reorganize the magnetic field into an approximately axisymmetric toroidal geometry. The MHD fluctuations that break the magnetic surfaces to allow the transport of current into the plasma (i.e., the plasma dynamo) also allow energy transport in the spheromak. If a favorable balance between current drive efficiency and energy confinement can be shown, the spheromak has the potential to yield an attractive magnetic fusion concept [2].

The magnetic fields and currents in the spheromak are nearly force free and satisfy the eigenvalue equation $\nabla\times\mathbf{B}=\lambda\mathbf{B}$, with $\lambda = \mu_0 J_{||}/B$ representing the locally normalized current density. The form of the field inside the flux conserver that satisfies the force-free condition and minimizes the total magnetic energy, the so-called *Taylor Relaxed State* with λ=const [3], allows for a stable equilibrium with arbitrarily large magnetic field and current density (that is, $J_{||}$ and B increase together) for a given coaxial source current. In principle, the spheromak current and field can grow until resistive dissipation balances the source input. Thus, it should be possible to generate the high fields and toroidal currents necessary to make the spheromak into a practical fusion reactor [4].

The spheromak buildup (the increase in field and current with time) resulting from an applied external source is commonly expressed in terms of the helicity balance:

$$\frac{dK}{dt} = 2V_g\Phi_g - \frac{K}{\tau_K} \qquad Eq.(1),$$

* Work performed under the auspices of the US DoE by University of California Lawrence Livermore National Laboratory under contract W–7405–ENG–48.

where the helicity $K=\int \mathbf{A}\bullet\mathbf{B}dV$, V_g is the voltage applied to the coaxial source electrodes which are linked by the vacuum magnetic flux Φ_g, and τ_K is the helicity decay time set by the ohmic dissipation $\int \mathbf{E}_\Omega\bullet\mathbf{B}\,dV$, with $E_\Omega=\eta J$. For the Taylor state, $\lambda=\lambda_{FC}=5/R_{FC}$, and $W_{mag}=\int B^2dV=\lambda K/2\mu_0$, so we see directly the connection between total helicity content and magnetic field strength. In this picture, the helicity (and magnetic field) builds until the helicity dissipation rate matches injection source rate. Typically, V_g is taken as given, but in fact, V_g is related to the spheromak parameters via the finite external circuit impedance. Furthermore, τ_K may not depend on the plasma resistivity alone. Thus, it may be difficult to predict the final state from the helicity balance determined early in the discharge.

In the remainder of this paper, we consider magnetic field generation in the Sustained Spheromak Physics Experiment (SSPX) in light of this model for helicity balance. In Section 2 we review the operation of the SSPX spheromak, and in Section 3 we discuss helicity balance for SSPX. Section 4 covers magnetic field buildup, and we conclude in Section 5 with a discussion of other possible mechanisms that may limit magnetic field generation and current amplification, as well as possible future experiments to address the physics limiting the field buildup.

2. Spheromak Formation in SSPX

The SSPX device [5] produces 1.5 - 3.5 msec, 1m dia. spheromak plasmas with a plasma minor radius of 0.23m. Fig. 1 contains a cross section of SSPX showing the major hardware components along with a typical MHD equilibrium. DC coaxial helicity injection is used to build and sustain the spheromak plasma within the flux conserver. The vacuum flux configuration for the coaxial injector is quite flexible in SSPX, as shown with two examples in Fig. 2. A spheromak plasma is formed when we inject gas into the coaxial region and apply 6kV to the inner electrode (the discharge cathode). The resulting plasma is rapidly ejected into the flux conserver when the current rises above the ejection threshold after ~150μsec. Fig. 3 shows the timeline for two typical SSPX discharges: 3370 uses only the formation pulse, while 6937 is sustained at lower current using a second capacitor bank with pulse-forming network.

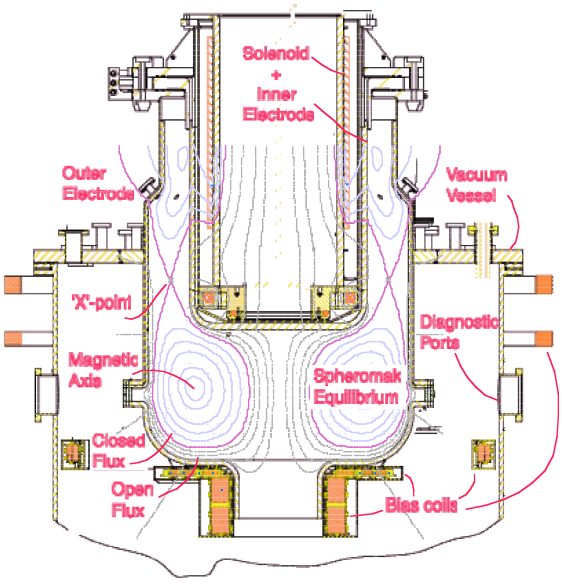

Fig. 1. SSPX cross section with MHD equilibrium from CORSICA.

The toroidal current and internal magnetic field profiles of the spheromak plasma are inferred from edge magnetic measurements using the CORSICA code to reconstruct the 2d MHD equilibrium for the force-free plasma. Peak toroidal currents of 0.75MA have been obtained so far, with peak edge poloidal fields of 0.3 Tesla. Electron temperature and density profiles are measured using a 10 channel Thomson scattering system and measurements of the Doppler broadening of impurity emission lines along a single chord provide a rough measure of the ion temperature [6]. We use the MHD reconstruction to compute the ohmic heating power from the measured T_e profiles and Z_{eff} determined from VUV spectroscopy.

In SSPX, we have used a combination of high temperature baking (165C), hydrogen glow discharge cleaning, helium discharge conditioning, and titanium gettering every 3-4 discharges to produce clean plasmas with Z_{eff}~2. The plasma-facing surfaces of the copper flux conserver are tungsten-coated to reduce sputtering. Peak plasma temperatures over 150eV have been measured with our Thomson scattering system when we operate near the sustainment threshold current to minimize magnetic field fluctuations. Under these conditions, the core electron thermal diffusivity (χ_e = 30m^2/sec) approaches tokamak L-mode values [7].

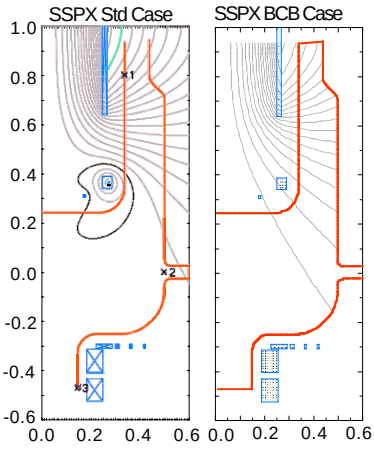

Fig.2. Representative vacuum flux configurations for SSPX.

Electron temperature data from a number of discharges, shown in Fig. 4, point to another reason for increasing the magnetic field strength in SSPX. Here we plot the core electron temperature vs. the core electron density normalized by B^2 (we note that most of the variation on the horizontal axis lies with n rather than B). The data appear bounded by a limiting electron pressure corresponding to β_e=3.5%, which is significantly higher than the Mercier limit computed using CORSICA [5]. Detailed comparison against predicted stability limits with realistic magnetic geometry (e.g., as with the DCON code [8]) awaits measurement of the local ion temperature, which chord-average data suggests is comparable to T_e.

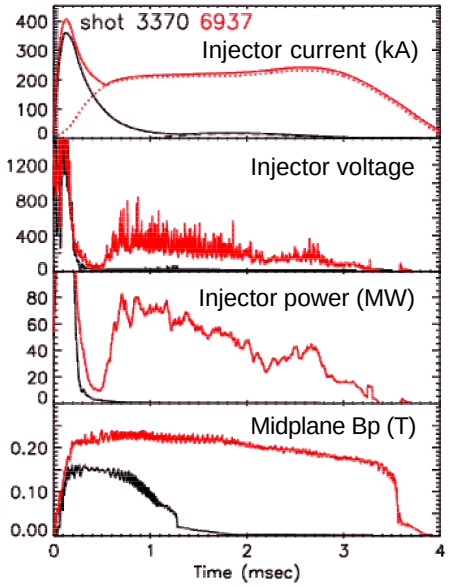

Fig.3. Representative discharges. 3370 -formation only, 6937-with sustainment bank.

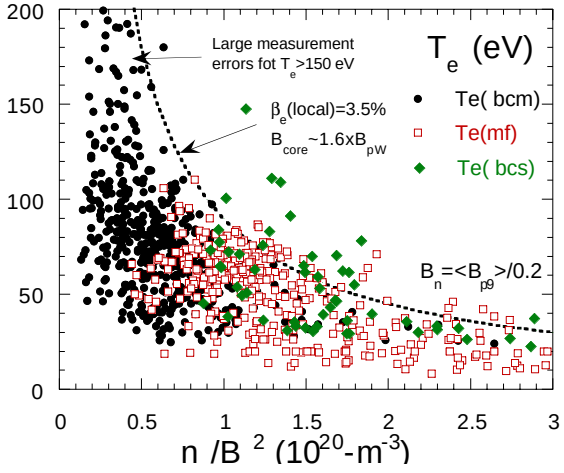

Fig.4. Core T_e vs. n_e/B^2. BCM and BCS are with bias coils, MF is without.

3. Helicity balance

In principle, helicity balance offers a simple way to analyze coaxial injection because, unlike energy, relaxation processes conserve helicity. However, the commonly-used Eq. (1) does not contain an explicit coupling coefficient between the coaxial injector and the spheromak; rather, it is buried in the individual components. For example, changes in the current distribution on the injector electrode affect the gun voltage, where and how rapidly helicity is dissipated, and may change the nature of the instabilities available for transporting

helicity from the edge to the core plasma. Also, the existence of a sheath in front of the electrodes will reduce the effective helicity injection rate.

We examine the helicity balance in SSPX by dividing the flux conserver volume into two regions: an edge volume with open field lines which carries the gun current, and a closed-flux spheromak core. The total helicity within the edge and spheromak core volumes is $K \approx K_{edge} + K_{core}$. Using Ohm's law and separating out ohmic dissipation and helicity transport (helicity flow) terms, the helicity balance in each volume is,

$$dK_{edge}/dt = 2\Phi_g(V_g - V_{sh}) - 2\int_{edge} \eta j_{\|} B_{\|} d^3r - (dK/dt)^{flow}_{ed-core} \qquad \text{Eq.(2a)},$$

$$dK_{core}/dt = (dK/dt)^{flow}_{ed-core} - 2\int_{core} \eta j_{\|} B_{\|} d^3r \qquad \text{Eq. (2b)},$$

where $(dK/dt)^{flow}_{ed-core}$ represents the dynamo term transporting helicity across the separatrix between the edge and the spheromak core volume. In the core plasma the dynamo term drives current to sustain the plasma against energy transport losses and decay by ohmic dissipation that heats the plasma. The relative magnitudes of the helicity transport term and the resistive decay rate determine buildup or decay of helicity in the spheromak. To apply Eq. 2 to the experiment, knowledge of the gun voltage, the gun flux, the sheath voltage drop, the plasma resistivity, the helicity content, and the plasma currents and magnetic field are needed.

The injector flux, Φ_g, is defined as that fraction of the initial vacuum flux which links the spheromak down the central column, as shown in Fig. 1. This fraction, typically 70-80% of the total flux produced by the injector solenoid, depends on the vacuum field geometry and on where electrical breakdown occurs in the coaxial region. The actual value is determined from the experimental MHD equilibrium. Were we to use the total vacuum flux connecting the electrodes, we would be including flux (about 20-30% of the total) that remains within the coaxial source region and does not contribute to building helicity in the core spheromak. In principle, we could include it, but would then have to define yet a third region over which to evaluate the ohmic dissipation term, and little is known about the plasma conditions far up in the coaxial source.

The injector voltage in Eq. (1), V_g, is actually comprised of three components: sheath, ohmic, and inductive, $V_g = V_{sh} + IR + L dI/dt + I dL/dt$ (note that the inductive terms represent not only global changes in current path, the net effect of fine scale magnetic turbulence which moves field lines). In Eq. (2), we explicitly subtract off the sheath voltage because helicity added to the sheath is dissipated immediately. The remaining voltage is available for building and sustaining the spheromak helicity. When driven near the sustainment threshold, the fluctuations are small and the gun voltage is low, 500V or less, and subtracting the sheath voltage introduces a significant correction to the helicity balance. We estimate the sheath voltage to be about 100V based on threshold voltage analysis and electrode heating.

Following the methods outlined above, we obtain reasonable helicity balance for SSPX discharges using measured quantities, finding in some cases that the sheath voltage introduces a significant correction. The ohmic dissipation is computed using temperature profiles from Thomson scattering and Z_{eff} from spectroscopy, along with the current density from the MHD reconstruction. During the formation phase, we can match the rise in spheromak helicity with the measured inputs: data from a magnetic probe in the injector confirms the fraction of flux pulled out of the coaxial source. In sustained plasmas driven with injector currents near threshold to keep magnetic fluctuations low, the gun voltage is low (< 500V), ohmic dissipation accounts for about 20% of the helicity input, and the sheath loss is the major

component of the helicity balance, as shown in Figure 5. In this case, we see that only a small fraction of the helicity input is available for building plasma current and magnetic field, though it is less than the ohmic dissipation, yielding a slow decrease in helicity content with time.

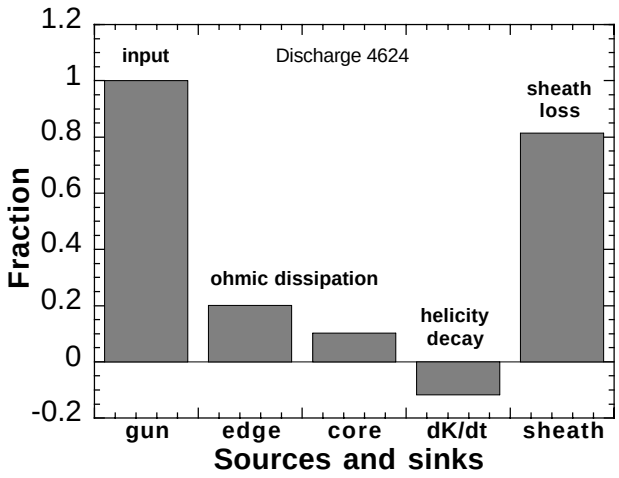

Fig. 5. Helicity balance for a group of nearly sustained SSPX discharges.

4. Magnetic field generation and buildup

It is often assumed that the maximum field strength in the spheromak is governed solely by a simple helicity balance dominated by ohmic dissipation with a given fixed applied voltage. When driven near threshold, we have shown that the electrode sheath can significantly reduce the net helicity input rate, making resistive losses even more important in determining the field buildup rate. Simple analysis and numerical simulation using CORSICA both show that, for a fixed parabolic electron temperature profile, dissipation inside the magnetic separatrix dominates the ohmic losses as the toroidal current and edge magnetic field increase. Thus, we might expect that hotter plasmas would allow generation of higher magnetic fields since $\eta \propto ZT_e^{-3/2}$. Instead, we find that the maximum edge poloidal magnetic field is almost independent of either the measured core or edge electron temperature over the range 30-150eV. These results suggest that there may be other mechanisms limiting the magnetic field generation, implying that the measured voltages do not represent much "dynamo action" transferring helicity to closed surfaces.

The complete ensemble of SSPX discharges show that the edge poloidal magnetic field (and thus the toroidal current) are strongly coupled to the injector current. These data appear in Fig. 6, where we plot the peak midplane edge poloidal field vs. the peak injector current. Typically, the injector current peaks during the initial formation phase and the midplane field peaks about 100μsec later. After this, the injector voltage falls to low values and the steady current supplied by the sustainment bank maintains the edge poloidal field near its peak value for another 1-2msec. There is a clear upper bound to the magnetic field data corresponding to $B_{pol}(T)=0.6I_{gun}(MA)$. This limit does not depend on the intial vacuum flux configuration and it is very close to the value of the toroidal field inside

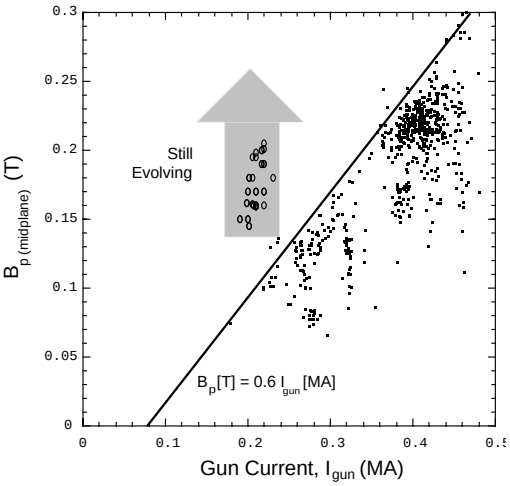

Fig. 6. Edge field scaling with I_{gun} for fast formation plasmas (dots), and for the steady build-up cases (circles).

the coaxial source, $B_{tor}(T)=0.5I_{gun}(MA)$, which suggests that spheromak field buildup might be limited by a dynamic pressure balance between the plasma in the injector ($\rho v^2+B_t^2/2\mu_0$) and the spheromak ($B_p^2/2\mu_0$), much like the condition for successful CT injection into tokamaks. Or maybe there is no reconnection at the throat of the injector so we just maintain the bubble-burst condition first outlined by Turner.

Recently, we added an external pulse-forming network to the sustainment bank to flatten and extend the current pulse so that we could look for sustained buildup at lower net helicity input rates (nearer threshold). When we operate with this bank alone (no large formation pulse like that in Fig. 2) we can produce a continuous buildup of helicity. At this point, we have almost twice the magnetic field per MA of gun current than with the early high current formation pulse. The gradual buildup in magnetic field and helicity content, so far limited only by the pulse length as shown in Fig. 7, is accompanied by large fluctuations in injector voltage producing a large time-average helicity injection rate $dK/dt \propto (V_{inj}-V_{sheath})$. This buildup occurs with or without the large n=1 magnetic fluctuations previously associated with spheromak buildup [9]. In some cases, we can correlate the voltage fluctuations with changes in edge poloidal fields, but usually there is little correlation, suggesting short scale-length magnetic fluctuations are responsible for the buildup. Planned measurements in the injector region, including fast imaging, should confirm whether the reconnection and helicity injection in these discharges occurs at the mouth of the injector, along the central column, or more uniformly around the plasma boundary.

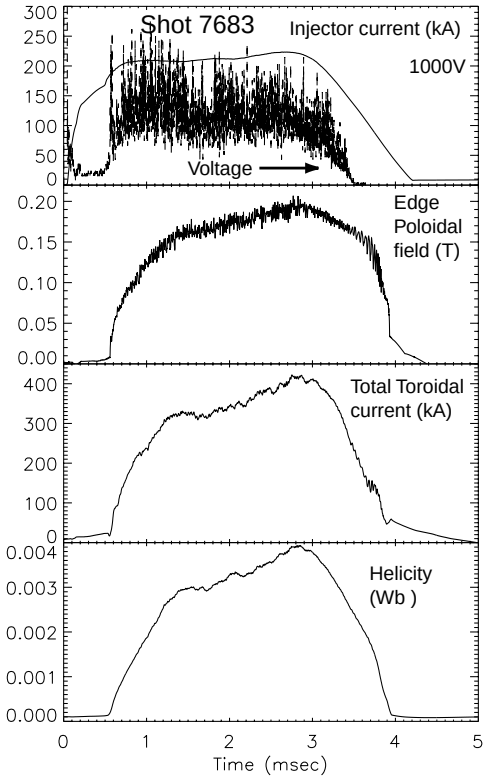

Fig.7. Slow buildup with steady injection.

5. Discussion and summary

The stiff relationship between magnetic field (and thus toroidal current) and injector current in the SSPX spheromak, independent of the initial vacuum magnetic field configuration or electron temperature in clean plasmas (Z_{eff} <3), suggests that the field amplification is not limited by helicity balance and a simple ohmic τ_K. The near equality of the toroidal field in the coaxial region to the spheromak edge poloidal field points to a limiting dynamic pressure balance and a possible lack of reconnection and formation of an x-point at the mouth of the injector. We plan to install magnetic probes in the injector to confirm the presence of an x-point by looking for field reversal on either side of it.

We speculate that it may also be that the current path changes rapidly during the course of a discharge; e.g., current begins flowing from the end of the inner electrode rather than from inside the coaxial region. Even though the vacuum magnetic field lines are frozen in place by the flux conserver, the current flow on them can change rapidly due to changes in local recycling or sputtering which affect the ion saturation current. The current path can change the helicity injection rate if one configuration is more unstable to kinking or

susceptible to reconnection than other. Kinking or reconnection can increase the helicity content of the plasma because they change the inductance - simple resistive voltage drops don't increase helicity content because the loss just matches the source. We plan to look for changes in the current distribution on the electrodes using fast imaging (100ns exposure times), magnetic probe arrays inserted into the coaxial region, and distributed heat flux measurements on the flux-conserver.

In parallel with the experimental effort to understand the mechanisms responsible for current drive in the spheromak, we are employing numerical simulation using the 2d CORSICA and 3d NIMROD codes. We modified Ohm's Law in CORSICA to include current diffusion due to magnetic turbulence. This "hyper-resistivity" model for Ohm's Law takes the form: $\mathbf{E}+\mathbf{v}\times\mathbf{B}=\eta\mathbf{j}-\left(\mathbf{B}/B^2\right)\nabla\cdot\left(\Lambda\nabla\lambda\right)$, where $\lambda=\mu_0\mathbf{j}\cdot\mathbf{B}/B^2$ and Λ (assumed spatially uniform here) is a measure of the current diffusion rate. We find that this model can reproduce the discharge current and 2d equilibrium parameters using the measured Te profiles. With NIMROD [10] we are simulating how the magnetic fields evolve in time and space inside the flux conserver after initial breakdown. The code predicts edge poloidal fields and internal q-profiles in qualitative and quantitative agreement with experiment, though the spectrum and amplitude of higher order modes may differ significantly. NIMROD consistently shows that most of the field lines make only a few toroidal transits within the flux conserver, which appears to be inconsistent with measurements showing T_e a flux function peaked at more than 120eV on the magnetic axis. Therefore, we are working to implement energy transport using Spitzer resistivity and realistic parallel and perpendicular thermal conductivities to compute the expected electron temperature profiles. Further details of these activities may be found in Ref. [11].

Clearly, it would be advantageous to increase the injector voltage well above the sheath voltage, thereby effectively using the energy in the capacitor bank to build up the spheromak magnetic field. The injector voltage depends on the supply voltage, external circuit impedance, and the internal impedance of the coaxial gun. The impedance of the SSPX injector is often much smaller than was observed in CTX, as shown in Fig. 8, which plots the measured injector voltage vs. current. At its highest values, the SSPX injector impedance is consistent with the $1/r_e$ dependence proposed by Barnes [12] (r_e is the mean radius in the coaxial region). Though not explained by Barnes, this dependence on radius may be an inductive effect correlated with the expulsion of plasma (and entrained flux) from the coaxial injector.

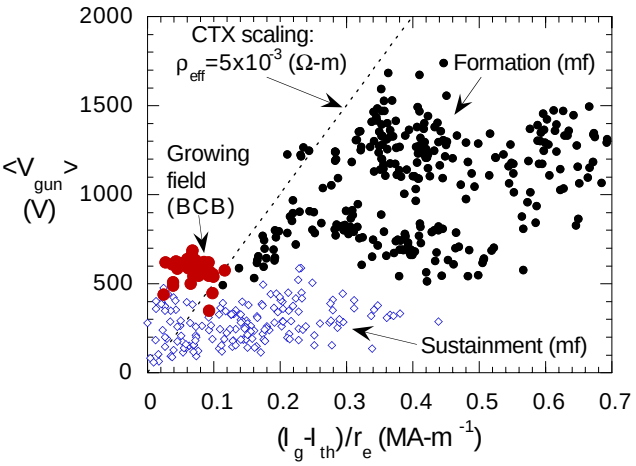

Fig. 8. SSPX gun voltage vs. current normalized by injector radius.

We are now examining two possible ways to increase the injector voltage on SSPX. First, we are considering reducing the external impedance of the power supply by replacing the pulse-forming network with a modular capacitor bank in which a number of high current switches are fired in sequence to produce a relatively flat, variable amplitude current pulse. Removing the inductor will increase the voltage on the injector and improve the energy coupling efficiency by better matching source and load impedances.

We are also considering adding a second, small diameter coaxial injector mounted in the divertor region opposite the existing injector (refer to Fig. 1). The smaller radius should increase the injector voltage if the impedance scales like $1/r_e$. We can then look for a faster rise in helicity content consistent with the helicity balance and we can see if there is a corresponding rise in maximum helicity content. We can also see if the maximum spheromak poloidal field again matches the toroidal field in the coaxial region. In addition, design changes made possible by the smaller diameter inner electrode will mean that we can instrument it to measure the current distribution throughout the discharge.

We anticipate that the higher spheromak magnetic fields and currents resulting from the modifications now being considered should provide direct evidence of whether the core plasma temperature is governed by radial transport, parallel transport on chaotic field lines ($T_e \propto V_g$ according to Ryutov [13]), or a pressure limit. Should the electron temperature increase significantly, it will provide further information on the relative importance of resistive dissipation and helicity balance to controlling the buildup of spheromak magnetic fields.

Acknowledgements

The authors wish to acknowledge helpful discussions with Ken Fowler and M. Nagata of the Himeji Institute of Technology (who also provided help with the ion temperature measurements). We would also like to acknowledge the competent technical support of R. Geer, J. Jolly, R. Manahan, N. Martovetski, and R. Kemptner.

References

[1] T. R. Jarboe, Plasma Phys. and Control. Fusion **36** 945 (1994)

[2] E. B. Hooper, *et al.*, Fusion Tech. **29** 191 (1996)

[3] B. Taylor, Rev. Mod. Physics **58** 741 (1986)

[4] T. K. Fowler, *et al.*, Fusion Tech. **29** 206 (1996)

[5] E. B. Hooper, L.D. Pearlstein, and R.H. Bulmer, Nuclear Fusion **39** 863 (1999)

[6] H. S. McLean, S. Woodruff, *et al.*. Rev. Sci. Instr. **72**, 556, (2001).

[7] H. S. McLean, S. Woodruff, E.B. Hooper, *et al*., Phys. Rev. Lett. **88** 125004 (2002)

[8] A.H.Glasser LANL report LA-UR-95-528, February 1995

[9] S. Woodruff, D.N. Hill, *et al.*, *A new mode of operating a magnetized coaxial gun for injecting magnetic helicity into a spheromak*, UCRL-JC-148201, June 2002, Submitted to Phys. Rev. Lett.

[10] A.H. Glasser, C.R. Sovinec, R.A. Nebel, et al., Plasma Phys. Cont. Fusion **39**, 715 (1997)

[11] R.H. Cohen, H.L. Berk, B.I. Cohen, *et al.*, paper TH/P2-01, these proceedings

[12] C. W. Barnes, *et al.*, Phys. Fluids B **2** (8) 1871 (1990)

[13] R.H. Cohen, E.B. Hooper, D.D. Ryutov, *Joule Heating of the Plasma on Open Field Lines*, UCRL-IR-147988, April 2002.